Manufacturing Letters 40 (2024) 164–167

Contents lists available at ScienceDirect

Manufacturing Letters

journal homepage: www.elsevier.com/locate/mfglet

Full Length Article

Impact of deposition time per layer in large format additive manufacturing with glass fiber reinforced ABS

Pablo Castelló-Pedrero *, César García-Gascón, Javier Bas-Bolufer, Carles Alabort-Martínez, Juan A. García-Manrique

Design and Manufacturing Research Institute, Universitat Politècnica de València, Valencia, Spain

ARTICLE INFO

Article history:
Received 1 March 2024
Received in revised form 14 April 2024
Accepted 29 April 2024
Available online 11 May 2024

Keywords:
Large format additive manufacturing
Adhesion
Composite materials
Thermomechanical analysis

ABSTRACT

This paper presents a parametric study of layer adhesion in Large Format Additive Manufacturing (LFAM) applications using glass fiber (GF) reinforced acrylonitrile butadiene styrene (ABS). The study focuses on the deposition time per layer (t_L) and includes an innovative approach to monitor temperature variation throughout the printing process using an infrared camera. The paper provides a detailed account of the sample fabrication process and experimental tensile tests. Specifically, this study shows how lower times per layer yield better mechanical properties as material is deposited over hotter layers, resulting in smaller thermal gradients, hence better layer adhesion and reduced warpage.

1. Introduction

LFAM is becoming increasingly important in industries like the aerospace, automotive [1] or naval [2], where there is a need to manufacture substantially large and complex components, considering the required tolerances. Additionally, the use of composite materials in material extrusion (MEX) processes is enabling the manufacturing of tougher and stiffer, but lighter, structures. Fiber load in a polymeric based matrix increases some mechanical properties [3,4].

However, the main issue with Additive Manufacturing (AM) at larger scales is warpage. As a consequence from the thermal gradients between adjacent layers, residual stresses are generated throughout the 3D printing process, causing the distortion of parts. One of the main reasons causing this undesired phenomenon is insufficient layer adhesion [5] due to an inefficient melting of the material, that produces temperature fluctuations at the print layer [1]. This weak adhering between layers leads to weaker structures, unable to withstand the thermal forces generated during the AM process, resulting in the dimensional distortion of 3D printed parts. Therefore, its truly important to understand the printing conditions affecting on obtaining an optimal layer adhesion in LFAM, hence avoid warpage in a high degree.

There are many factors that affect adhesion between adjacent layers in 3D printed bodies. As studied previously, extruder and bed temperatures, layer width and height, and chamber temperature, are identified as some of the main conditions affecting layer adhesion [6–10]. In this paper, the material deposition time per layer (t_L) is the factor to be studied, as it is known that a minimum time per layer is needed for a correct adhesion [11]. Aliheidari et al. [6] studied the interlayer adhesion of double cantilever beam (DCB) specimens of acrylonitrile butadiene styrene (ABS) printed under different conditions. Rodzen et al. [7] proposed printing under favorable crystallization conditions, varying chamber temperature, to improve the layer-layer adhesion in FFF 3D printed PEEK/CF, for injection molding. On its side, Spoerk et al. [9] concluded that an optimal adhesion is achieved by printing parts with bed temperatures slightly over the glass transition temperature (T_g), when PLA and ABS is used.

More specifically, regarding studies related to LFAM, Duty et al. [11] analyzed the mechanical properties of specimens printed in ABS and other composite materials, such as CF-ABS, using a big area AM (BAAM) machine. Hassen et al. [12] also uses a BAAM system to characterize the mechanical and thermal properties of PPS with different percentages of CF reinforcement. Also concerning PP-based filament materials, Spoerk et al. [10] concluded that warpage in LFAM could be reduced by enhancing adhesion to the printing plate by increasing the platform roughness and temperature, and with higher flow rates.

Therefore, this research work proposes a parametric study of t_L with an innovative focus on the temperature evolution of layers along the complete LFAM process. The objectives of this research

* Corresponding author.

https://doi.org/10.1016/j.mfglet.2024.04.002

work include to study the effect of the printing time per layer on adhesion and, subsequently, the mechanical properties related to bodies printed in ABS with 20% GF reinforcement (ABS/GF20). Experimental tensile testing is going to be performed to study the strength force between layers, as it is strongly correlated with layer adhesion quality.

2. Materials and methods

The composite material studied in this work is composed of an ABS matrix with small GF reinforcements (ABS/GF20). It is industrially known as PolyCoreTM ABS-5012, commercialized in pellets form, featured with great cost effectiveness and excellent printability, designed for LFAM applications, and T_g = 96 °C [13].

The study was conducted with a personalized LFAM machine, named SuperDiscovery 3D by CNC Barcenas (Valdepeñas, Spain). This 3D printer is focused on large format fused granulate fabrication (FGF), using pellets extrusion and allowing an increased material flow rate.

Part of the study involve temperature measurements along the LFAM process, hence Optris PI640 (Berlín, Germany) is used. With an optical resolution of 640x480 pixels, it delivers pin-sharp radiometric pictures and videos in real time. The main thermal specifications [14] show that the printing temperatures in the study are within the working range of the camera (0 °C to 250 °C). The infrared camera was located inside the printing chamber, as shown in Fig. 1a. Together with a thermography software, it allows the observation of temperature fluctuations along time within layers, as well as the calculation of thermal gradients between adjacent layers, computed in Python v3.13 (Python Software Foundation) from snapshots (Fig. 1(c-d)).

To investigate the effect of deposition time per layer (t_L), it should be kept as a variable, while the rest of 3D printing parameters are constant. Printing settings are summarized in Fig. 1b, whilst t_L is set to 20, 30, 40, 50 and 60 s, during the 5 cases studied, summarized in Fig. 3b. Additionally, for a fair test, atmospheric conditions are controlled along the different tests by holding closed the printing chamber, to maintain a fairly constant atmospheric temperature and pressure.

The geometry of the printed specimen is shown in Fig. 2a, based on a standardized oval cross-section hollow prism. Cura 3D software (Ultimaker B.V., Utrecht, The Netherlands) is used to set the printing conditions for each oval prism specimen. Later, tensile testing specimens will be manufactured from both flat sides.

To investigate the adhesion between layers, a series of tensile tests are designed. A total of 30 specimens (Fig. 2b) are tested, 6 per t_L case. The specimens are manufactured by water jet cutting through the flat parts of the printed oval hollow specimens, as shown in Fig. 2c. Water jet cutting allows quick manufacturing, high accuracy, and perfect surface finishing. The specimen geometry is within the standard ASTM D638 Type I [15] (Fig. 2c), with an average thickness (t) of 5.5 mm.

A universal mechanical testing machine is used to perform the tensile tests (Fig. 2d). Atmospheric conditions are kept constant during all the test, performed at room temperature (25 °C approximately). Specimens are clamped at the same point and a strain rate of 5 mm/min is applied in each case, to ensure a fair test.

Once data, related to force (F) and extension (Δl), is obtained from the tests, stress (σ) and strain (ϵ) are calculated. Strain is simply the relationship between the total length of the specimen and the extension, so could be calculated by $\epsilon = \Delta l/L$. On the other hand, stress is calculated using $\sigma = F/wt$, where w and t corresponds to the width and thickness.

3. Results and discussion

Tensile testing experimental results are plotted and key points are summarized in Fig. 3. A strain–stress plot is shown in Fig. 3a where, directly, a clear elastoplastic (but brittle) behavior can be appreciated for every case. Initially, due to a correct adhesion between layers, an elastoplastic behavior is observed. Because of proper fusion between layers, the material is deforming. However, as strain increases, a brittle behavior is observed due to failure in the adhesion between layers, as it was expected. Fig. 3a allows a comparison between the different cases studied.

Moreover, results in Fig. 3b show a clear trend: strain at failure reaches a maximum at t_L = 30 s, gradually decreasing as t_L increases. Similarly, maximum average fracture stress is obtained

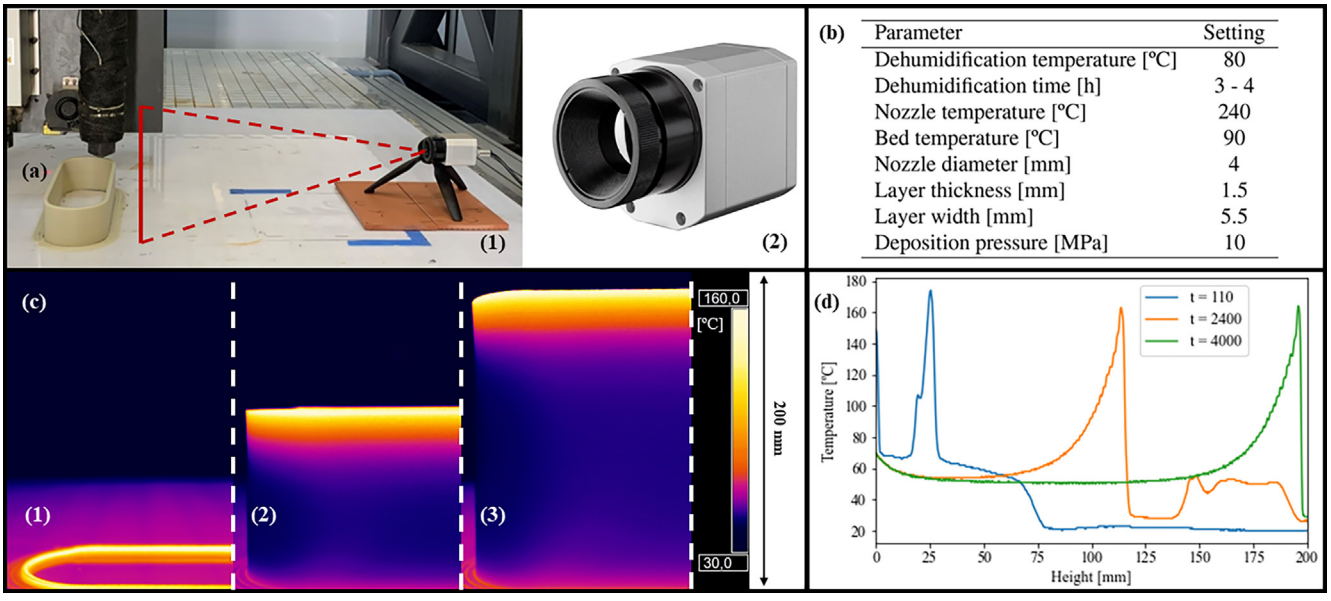

Fig. 1. (a) Infrared camera: (1) location with respect to the printing area, red lines show the capture area, and (2) model Optris PI640 [14]. (b) Summary of printing parameters set for the LFAM process. (c) Snapshots of thermal camera output video for t_L = 30, at instants: (1) t = 110 s, (2) t = 2400 s, and (3) t = 4000 s. (d) Evolution of temperature along height for the same time instants.

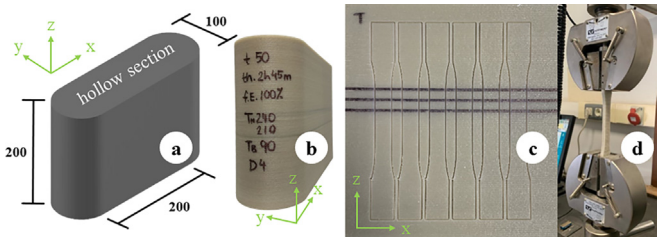

Fig. 2. (a) Standardized hollow geometry designed for the study. (b) 3D printed oval prism sample. (c) Standard ASTM D638 Type I [15] specimens water cut from the material plate. (d) Tensile testing procedure.

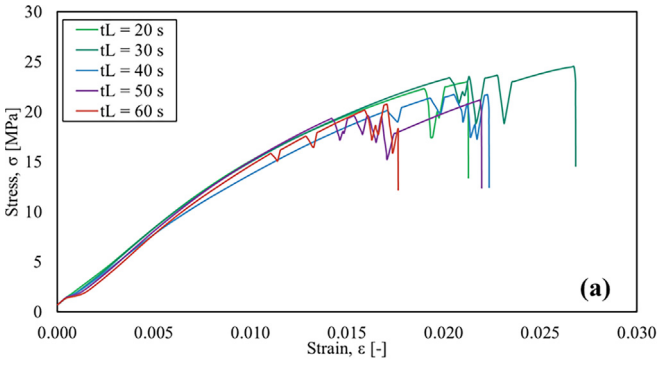

t_L [s]	20	30	40	50	60
N_v [mm/s]	34.76	23.17	17.38	13.90	11.59
σ_f [MPa]	19.81	19.92	18.69	19.59	19.30
ϵ_f [-]	0.019	0.022	0.020	0.016	0.015
E [GPa]	1.533	1.615	1.625	1.666	1.727

(b)

Fig. 3. (a) Stress–strain curve to compare the experimental results for each case. (b) Summary of results and key values for each case.

at t_L = 30 s, following a related trend for the rest of t_L values except for t_L = 40 s. However, E values increase as t_L increase. This means that with greater t_L, the structure is stiffer, however, it has a limited ability to absorb energy through plastic deformation, hence more prone to undesired sudden failure. Therefore, regardless the small differences, it could be concluded that the ideal deposition time per layer would be around 30 s, corresponding to a nozzle velocity (N_v) of 23.17 mm/s, at least for the printing conditions and the structure described.

The reasons behind these results are mainly related to the temperature of the layer over which the new layer is being deposited, called the top layer temperature at deposition. For greater t_L, the newly deposited layer has a greater time to cool down before the next layer is deposited on top. This means that, a lower t_L allows material to be deposited with a smaller thermal gradient between layers, favoring the adhesion between layers and decreasing warping of structures.

However, reducing too much t_L has been demonstrated to have adverse effects. Even though adhesion is performed at higher temperatures, structural defects like, layer skipping, appear due to a too high nozzle velocity. In addition, partial cooldown of the previous layer is preferred prior to the new deposited layer, to ensure the structure integrity and avoid deformations. Therefore, the results for t_L = 20 s, are not considered relevant for the study, as specimens break due to structural defects.

Furthermore, in Fig. 4, it can be observed the evolution along the height, of the temperature of the top layer just before the new layer is deposited. Fig. 4 shows how this temperature evolves along the build-up of layers, showing a clear decrease in temperature trend by the regression line. Layers closer to the printing bed

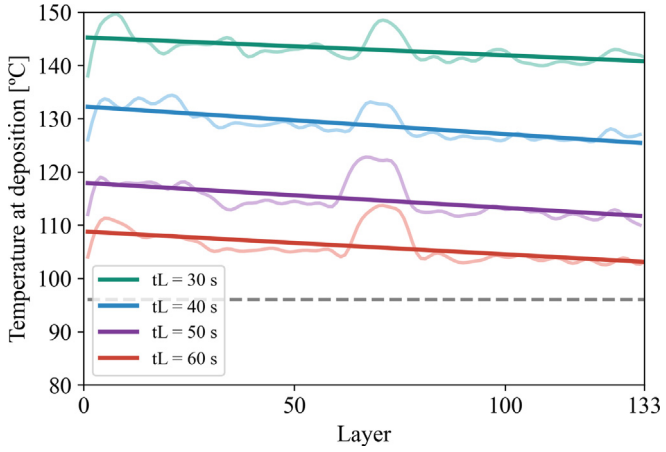

Fig. 4. Comparison of temperature of the previous deposited layer when the new layer is deposited. The regression lines of the real evolution of the temperature per layer are plotted for each case. The gray dashed line represents the T_g.

are deposited over a layer at a greater temperature, which decrease as higher layers are deposited, due to cooling down with exposition to the air and less influence from the bed. Comparing for different t_L cases, similar cooling rate rates are observed, which explain the decrease in mechanical properties as t_L increase. Highlight that every layer is deposited before the temperature of the previous layer falls below the T_g.

During the experimental testing, it was observed that 83.3% of the specimens fractured in the middle to top region. Attaining to the evolution of the top layer temperature at deposition in Fig. 4, the fracture region focuses at lower deposition temperatures, where adhesion is poorer.

4. Conclusions

This work presents a parametric study of layer adhesion in LFAM applications using GF reinforced ABS. An innovative methodology has been proposed to study the deposition time per layer (t_L). An infrared camera was used to record the thermal behavior of the structure along the deposition of layers. The paper includes a description of the manufacturing process of the specimens and the experimental tensile testing.

Despite the small differences between each case, the following conclusions can be raised from the parametric study regarding the t_L: (1) For t_L lower than 30 s, defects appear during the LFAM process, so results are excluded from thermal analysis. (2) σ_f and ϵ_f decrease as t_L increase, whilst E increases. (3) A t_L around 30 s is believed to be optimal in mechanical terms, as the structure showed a better ability to absorb energy through plastic deformation, hence less prone to sudden failure. (4) The evolution of the top layer temperature at deposition, along the build-up of layers, behave similarly for every layer deposition time, as expected. (5) A greater number of specimens break in the region of lower top layer temperature.

In general, greater mechanical properties are achieved with higher top layer temperatures prior to deposition, as layers are able to fuse more efficiently. ABS/GF20 is farther away from crystallization temperature, hence a greater quality layer adhesion is obtained with lower t_L. Therefore, during LFAM processes with ABS/GF20 an agreement between t_L and structure integrity should be achieved. As the methodology described in this paper has been applied successfully, as future work it is proposed to couple a complete parametric study on layer adhesion with numerical models.

Declaration of Competing Interest

The authors declare that they have no known competing financial interests or personal relationships that could have appeared to influence the work reported in this paper.

Acknowledgement

This work was supported by Generalitat Valencia (GVA) and Spanish Ministry of Science and Innovation. INVEST/2022/131, CIACIF/2021/286, TED2021-130879B-C21 and CIPROM/2022/3

References

[1] Shah J, Snider B, Clarke T, Kozutsky S, Lackil M, Hosseini A. Large-scale 3D printers for additive manufacturing: design considerations and challenges. Int J Adv Manuf Technol 2019;104:3679–93.
[2] Moreno-Nieto D, Casal-López V, Ignacio-Molina S. Large-format polymeric pellet-based additive manufacturing for the naval industry. Addit Manuf 2018;23:79–85.
[3] Love L, Duty CE, Post BK, Lind RF, Lloyd PD, Kunc V, Blue CA. Breaking barriers in polymer additive manufacturing, SAMPE, Baltimore, MD, USA, 2015.
[4] Wedgewood A, Pibulchinda P, Vaca EB, Hill C, Bogdanor MJ. Materials development and advanced process simulation for additive manufacturing with fiber-reinforced thermoplastics (Final Technical Report). United States, 2020.
[5] Bourell D, Kruth JP, Leu M, Levy G, Rosen D, Beese AM, Clare A. Materials for additive manufacturing. CIRP Ann 2017;66(2):659–81.
[6] Aliheidari N, Christ J, Tripuraneni R, Nadimpalli S, Ameli A. Interlayer adhesion and fracture resistance of polymers printed through melt extrusion additive manufacturing process. Mater Des 2018;156:351–61.
[7] Rodzen K, Harkin-Jones E, Wegrzyn M, Sharma PK, Zhigunov A. Improvement of the layer-layer adhesion in FF 3D printed PEEK/carbon fibre composites. Compos - A: Appl Sci 2021;149:106532.
[8] Yang C, Tian X, Li D, Cao Y, Zhao F, Shi C. Influence of thermal processing conditions in 3D printing on the crystallinity and mechanical properties of PEEK material. J Mater Process Manuf Sci 2017;248:1–7.
[9] Spoerk M, Gonzalez-Gutierrez J, Sapkota J, Schuschnigg S, Holze C. Effect of the printing bed temperature on the adhesion of parts produced by fused filament fabrication. Plast Rubber Compos 2018;47:17–24.
[10] Spoerk M, Gonzalez-Gutierrez J, Lichal C, Cajner H, Berger GR, Schuschnigg S, et al. Optimisation of the adhesion of polypropylene-based materials during extrusion-based additive manufacturing. Polym J 2018;10:490.
[11] Duty CE, Kunc V, Compton B, Post B, Erdman D, Smith R, et al. Structure and mechanical behaviour of big area additive manufacturing (BAAM) materials. Rapid Prototyp J 2017;23(1):181–9.
[12] Hassen AA, Lindahl J, Chen X, Post B, Love L, Kunc V, Additive manufacturing of composite tooling using high temperature thermoplastic materials, SAMPE (May 2016), Long Beach, CA, USA.
[13] PolyCoreTM ABS-5012, Polymaker, https://polymaker.com/polycore/ [accessed 10 December 2023].
[14] PI640i, Precision line, Infrared cameras, Optris, https://www.optris.com/en/product/infrared-cameras/pi-series/pi-640i/ [accessed 5 November 2023].
[15] ASTM D638-14. Standard Test Method for Tensile Properties of Plastics, ASTM International, USA, 2014. [accessed 23 May 2023]